ACCEPTED MANUSCRIPT
APL Materials
AIP Publishing
This is the author's peer reviewed, accepted manuscript. However, the online version of record will be different from this version once it has been copyedited and typeset.
PLEASE CITE THIS ARTICLE AS DOI:10.1063/5.0079195

Solution-processed thin film transistors incorporating YSZ gate dielectrics processed at 400•C

Giorgos Antoniou,[1] Nathan R. Halcovitch,[2] Marta Mucientes,[3] William I. Milne,[4] Arokia Nathan,[5] Judith L. MacManus-Driscoll,[6] Oleg V. Kolosov[3] and George Adamopoulos[1*]

[1] *Department of Engineering, Lancaster University, Lancaster LA1 4YR, UK*
[2] *Department of Chemistry, Lancaster University, Lancaster LA1 4YB, UK*
[3] *Department of Physics, University of Lancaster, LA1 4YW, UK*
[4] *Department of Engineering, University of Cambridge, 9 JJ Thomson Avenue, Cambridge CB3 0FA, UK*
[5] *Cambridge Touch Technologies, 154 Cambridge Science Park Milton Road, Cambridge CB4 0GN, UK*
[6] *Department of Materials Science and Metallurgy, University of Cambridge, 27 Charles Babbage Road, Cambridge CB3 0FS, UK*

Keywords: High-k dielectrics, solution-processed electronics, Yttria stabilized zirconia, spray pyrolysis, thin film transistors

ABSTRACT

This work investigates a solution process for yttria stabilized zirconia (YSZ) thin film deposition involving addition of yttria nanoparticles, at 400 °C, in air. Different yttrium doping levels in the YSZ were studied and a wide range of optical, structural, surface, dielectric and electronic transport properties were also investigated. An optimum yttrium doping level of 5 % mol. resulted in the smoothest films (R_{RMS} ~ 0.5 nm), a wide band gap (~5.96 eV), a dielectric constant in excess of 26, and leakage current of ~0.3 nA cm^{-2} at 2 MV/cm. The solution processed YSZ films were incorporated as gate dielectrics in thin films transistors with solution-processed In_2O_3 semiconducting channels. Excellent operational characteristics, such as negligible hysteresis, low operational voltages (5 V), electron mobility in excess of 36 cm^2 V^{-1} s^{-1}, high on/off current modulation ratio on the order of 10^7, and low interfacial trap density states (<10^{12} cm^{-2}) were

* Corresponding author. Email: g.adamopoulos@lancaster.ac.uk

APL Materials
ACCEPTED MANUSCRIPT
This is the author's peer reviewed, accepted manuscript. However, the online version of record will be different from this version once it has been copyedited and typeset.
PLEASE CITE THIS ARTICLE AS DOI:10.1063/5.0079195
AIP Publishing

demonstrated. Also, excellent film homogeneity was achieved over a large area (16 cm x 16 cm), with both film thickness and capacitance deviation of < 1.2%.

I. INTRODUCTION

Despite their short history, metal oxide-based thin film transistors (TFTs) have already been demonstrated with high charge-carrier mobilities[1-6] and an overall performance that is comparable to that of polycrystalline Si. Such metal oxide TFT technology enables the possibility of fabricating high-performance devices via scalable and potentially low-cost manufacturing processes for emerging applications in large-area microelectronics, particularly for the fast-growing IoT area.

High-performance metal oxide-based TFTs are usually manufactured using costly, vacuum-based processing methodologies. To address this problem, recent efforts have focused on the development of TFTs using alternative deposition methods based on solution processing paradigms.[7-16] However, research efforts towards the development of solution-processed dielectrics has been relatively slow, with most of the reported work performed using SiO_2 with only moderate performance and operation at relatively high voltages, thus consuming high power. In an effort to address problems of SiO_2 such a thermal stability, and high tunneling leakage currents when devices are downscaled, research efforts on high-k dielectrics, notably oxides, for SiO_2 replacement have attracted considerable attention.[17,18]

Such a replacement would need a relative dielectric constant, k, value in the range 25 to 30, as a much higher k values cause undesirably large fringing fields at the source and drain electrodes.[19] Additionally, to inhibit conduction by the Schottky emission of electrons or holes into the bands, the band-offset condition between the dielectric and the semiconductor channel needs to be greater than ~1 eV. Hence, a dielectric with a reasonably large band gap is necessary.[20] Oxide semiconductors typically have wide band gaps (>3 eV). Since the dielectric constant varies

APL Materials ACCEPTED MANUSCRIPT
AIP Publishing
This is the author's peer reviewed, accepted manuscript. However, the online version of record will be different from this version once it has been copyedited and typeset.
PLEASE CITE THIS ARTICLE AS DOI:10.1063/5.0079195

inversely with the band gap,[21,22] the choice of a suitable dielectric in metal oxide TFTs is quite limited. To get the right balance of band gap and k value, work has focused on ZrO_2,[23] HfO_2,[24] silicates,[18] and phosphates.[25] Among these, ZrO_2 and doped ZrO_2 has been most extensively studied. In particular, yttria-stabilized zirconia (YSZ) is of particular interest for MOSFET gate dielectric due to its high dielectric constant (25 - 29) and wide band gap (5.1 eV to 7.8). [26-28]

Partially (PSZ) or fully stabilized (FSZ) zirconia of the cubic phase can be achieved at relatively low temperatures, even at room temperature, by either heavy ion irradiation,[29,30] or the addition of aliovalent dopants to induce oxygen vacancies. To that end, oxides such as Y_2O_3,[31,32] CeO_2,[26,33-35] MgO,[36-42] Mn_3O_4,[43,44] and Sc_2O_3[45-47] have been used for full or partial ZrO_2 stabilization.

YSZ is most well-known for its high ionic conductivity at high temperatures,[48] extraordinary thermal and chemical stability, high hardness, mechanical durability and chemical inertness. Also, in its powder form it is used to make coatings that are chemically inert to mechanical wear and tear for applications in cutting tools.[49] There also has been a growing interest of YSZ in photonic applications,[50-53] in near-IR and mid-IR transparent window,[54] as buffer layer in silicon chip technology[55] and rarely as a gate dielectric. [26-28]

YSZ films can be grown by a variety of chemical and physical deposition methods[39], e.g. chemical vapor deposition (CVD),[56,57] atomic layer deposition (ALD),[58,59] sol-gel,[60-62] pulsed laser deposition (PLD), [63-66] and magnetron sputtering.[67-70]

Here we show that spray coating can be used to grow large-area-compatible YSZ thin film dielectrics for high performance TFTs, with excellent electron transport characteristics i.e. operating voltages of 5 V, negligible hysteresis, high on/off current modulation ratio, low leakage currents, tunable threshold voltage and electron mobility of ~ 36 cm^2 V^{-1} s^{-1}.

ACCEPTED MANUSCRIPT
APL Materials
This is the author's peer reviewed, accepted manuscript. However, the online version of record will be different from this version once it has been copyedited and typeset.
PLEASE CITE THIS ARTICLE AS DOI:10.1063/5.0079195
AIP Publishing

II. EXPERIMENTAL

A. THIN FILM DEPOSITION AND COMPOSITION

YSZ films with a range of yttrium doping levels were made by depositing different mixtures of zirconium(III) 2,4-pentanedionate and dispersed Y_2O_3 nanoparticles. The zirconium(IV) 2,4-pentanedionate (Alfa Aesar) was dissolved in methanol at a concentration of 38 mg/ml and was stirred at room temperature for about 5 hours to ensure complete dissolution of the precursor. The yttrium oxide nanoparticles of average particle size in the range between 25 and 40 nm (Sigma Aldrich) were dispersed in 0.1 M HCl acid to prepare a 30 mg/ml dispersion that was stirred at room temperature for 12 hours to ensure an agglomeration-free dispersion. Blends of the aforementioned solutions in different ratios (to result in different yttrium to zirconium ratios) were spray coated onto fused silica, glass and ITO-coated glass (sheet resistivity of 10 Ohms/sq.) substrates at 400 ºC using a pneumatic airbrush with a nozzle size of 0.3 mm. The airbrush was held at a vertical distance of about 30 cm above the substrate and after a 10 s spray coating period the spray process was interrupted for 60 s to allow the vapors to settle. The cycle was repeated until films of ~100 nm thickness were obtained. This process yielded the best film homogeneity over a 16 cm x 16 cm deposition area. For the TFT device studies that are described later in the manuscript, semiconducting channels of In_2O_3 were deposited onto the glass/ITO/YSZ stacks at 400 °C. The films were spray coated rom 0.05 M indium chloride ($InCl_3$) solutions in methanol and films of ~ 10 nm thickness were obtained.

Au and Al source and drain contacts for making the metal-insulator-metal devices from glass/ITO/YSZ and glass/ITO/YSZ/In_2O_3 stacks were thermally evaporated under high vacuum (10^{-7} mbar) through a shadow mask. The typical metal contact areas were ~ 0.01 mm^2 and thicknesses ~ 60 nm.

ACCEPTED MANUSCRIPT
APL Materials
AIP Publishing
This is the author's peer reviewed, accepted manuscript. However, the online version of record will be different from this version once it has been copyedited and typeset.
PLEASE CITE THIS ARTICLE AS DOI:10.1063/5.0079195

B. CHARACTERIZATION

UV-Vis absorption spectroscopy measurements of YSZ films on fused silica were conducted at wavelengths between 180 nm and 1000 nm using an Agilent Cary 5000. The microstructures of the YSZ films on ITO-coated glass was analyzed by Grazing Incidence XRD (GIXRD) experiments (with a grazing incidence angle of 0.6°) that were conducted using a Rigaku SmartLab diffractometer with CuK_α radiation operating at 45 kV and 200 mA, a Ge(220)x2 monochromator, and a DteX250 1D detector.

The surfaces morphologies of spray coated YSZ onto ITO-coated glass were characterized by contact mode atomic force microscopy (AFM) measurements undertaken in ambient conditions using a Bruker Nanoscope V system and Multimode low noise head using force modulation cantilevers. Also, to further investigate the stacks' interfaces ultrasonic force microscopy (UFM) measurements were carried out under the same conditions using a modified version of Bruker Nanoscope V system. The high resolution UFM measurements were performed using a 4.5 MHz carrier frequency and 2.7 kHz modulation frequency with deflection signal acquired via custom-built interface. Prior to UFM, the /ITO/YSZ/In_2O_3/Al stacks underwent Beam-Exit Cross-Sectional Polishing (BEXP) on an angled holder (3° slope) with an overhang of ~300 μm. The beam entry surface was then filed down normal to the beam direction with decreasing size 30 μm through a 1 μm diamond impregnated film. The holder was placed within the vacuum chamber and beam-exit cross-sectional polishing was initiated at a vacuum of 2.0×10^{-5} mbar at a 7 kV accelerating voltage for 10 hours followed by 1 kV for 15 min polishing. Once beam-exit occurred, the voltage was decreased to 1 kV for 20 min to polish the surface. The process resulted in a near-atomically flat cut at approximately 11° through the area of interest with respect to the sample surface through the area of interest. Prior to scanning probe imaging, samples were cleaned in an ultrasonic bath using acetone and methanol for 10 minutes and dried with nitrogen.

ACCEPTED MANUSCRIPT
APL Materials
This is the author's peer reviewed, accepted manuscript. However, the online version of record will be different from this version once it has been copyedited and typeset.
PLEASE CITE THIS ARTICLE AS DOI:10.1063/5.0079195
AIP Publishing

Admittance spectroscopy measurements on Metal-Insulator-Metal stacks (i.e. glass/ITO/YSZ/Al) for different Y_2O_3 to ZrO_2 molar ratio were performed using a Wayne Kerr 6550B precision impedance analyzer at frequencies between 1 kHz and 50 MHz applying a 25 mV AC voltage. Bottom-gate, top-contact thin film transistors characterization was carried out under vacuum (10^{-3} mbar), at room temperature using an Agilent B1500A semiconductor parameter analyzer. Device parameters including electron mobility and interfacial trap density were extracted from the transfer curves in both the linear and saturation regime using the gradual channel approximation.

III. RESULTS AND DISCUSSION

The band gaps of the YSZ films were determined by Tauc plots, as illustrated in **Figure S1.** The plots indicate a direct band to band transition for the different yttrium doping levels. **Figure 1a** shows that the fundamental absorption edge of the YSZ films shifts from 5.76 eV to 5.95 eV with an increase of the yttrium content up to a maximum for an yttrium doping level of about 5 mol.% indicating a cubic phase of YSZ.[71]

The linear dependence in the semi-logarithmic representation (**Figure S1**) reveals an Urbach-type behavior, as previously reported for YSZ.[72] An Urbach-type behavior is attributed to a structural or thermal disorder causing an exponentially decaying density of localized states at the band edge. **Figure 1b** clearly illustrates the increase of the structural disorder with increased yttrium doping levels, as previously reported for YSZ.[73] An increase in structural disorder has been linked to a reduced number of oxygen vacancies in the ZrO_2 lattice[72,74] and hence this is expected here for high yttrium doping levels.

The XRD diffraction patterns of YSZ films on ITO-coated glass with different yttrium doping levels is depicted in **Figure 2a**, whereas those on c-Si are illustrated in **Figure S2**.

ACCEPTED MANUSCRIPT
APL Materials
AIP Publishing
This is the author's peer reviewed, accepted manuscript. However, the online version of record will be different from this version once it has been copyedited and typeset.
PLEASE CITE THIS ARTICLE AS DOI:10.1063/5.0079195

XRD patterns of the different composition YSZ films show the co-existence of both tetragonal and cubic phases as evidenced by the presence of two well-discriminated peaks at about 2θ=30.8° and 2θ=31.5° characteristic of tetragonal (JCPDS 83-113) and cubic (JCPDS 82-1246) ZrO_2 respectively. A monotonic increase of the (111) reflection, characteristic of cubic ZrO_2 is observed with increasing yttrium doping level up to 5 mol.%[75] Plotting relative intensity ratio of this (111) reflection from the cubic phase to the tetragonal (011) peak (**Figure 2b**), confirms that the cubic phase of YSZ dominates up to ~5 mol% yttrium doping. As observed in **Figure 2b** the fraction of cubic ZrO_2 is inversely correlated with the average crystal size as has been shown before.[76] Similar results were found for YSZ films that were simultaneously spray coated on c-Si (**Figure S2**).

Selected friction raw images of the YSZ films after average signal subtraction are presented in **Figure 3a, 3b and 3c**. The related topography images are shown in the insets **Figure 3a, 3b and 3c**. The root-mean-square roughness of the film surfaces were found to be of ~1.4 nm, ~0.5 nm, and ~0.4 nm for YSZ films with yttrium doping level of 0 mol.%, 5 mol.% and 15 mol.% respectively, indicating that surface morphology and growth are dominated by the deposition conditions rather than the surface morphology of the underlying ITO whose surface roughness is ~1.4 nm.

Figure 3d, 3e and **3f** provide further insights on the film microstructures and interfaces. Notably, pure ZrO_2 films (**Figure 3d**) shows a laminar structure. Such features however are less evident for YSZ films with higher yttrium doping level (**Figure 3e** and **3f**). Also, the quality of the interface between the YSZ and ITO (**Figure 3f**) deteriorates at high yttrium content and this degrades the device performance, as we show later. Nevertheless, the inset in **Figure 3d, 3e** and

APL Materials ACCEPTED MANUSCRIPT
AIP Publishing
This is the author's peer reviewed, accepted manuscript. However, the online version of record will be different from this version once it has been copyedited and typeset.
PLEASE CITE THIS ARTICLE AS DOI:10.1063/5.0079195

3f, showing the TFT device cross-section (glass/ITO/YSZ/In_2O_3/Al) UFM images, reveals clear interfaces between the YSZ films and the ITO with yttrium doping level up to 5 mol. %.

Investigations of the nanomechanical properties of the films using UFM showed significantly higher effective elastic modulus of the YSZ film with yttrium doping level of 5 mol % compared to the pure ZrO_2. This confirms stabilization of the stiffer cubic phase of ZrO_2 with 5 mol. % yttrium doping as has theoretically been predicted before.[75,77] However, more detailed analysis is outside the scope of the present study.

Susceptance and conductance dispersions as well as Nyquist plots in the frequency range between 1 kHz and 15 MHz of representative YSZ dielectrics in metal-insulator-metal devices are illustrated in **Figure S3**. The plots reveal stable systems whose equivalent circuit consists of a capacitor with high shunt and low series resistances.

The geometric dielectric constant at 1 kHz (calculated from Bode plots that are shown in **Figure 4**) as a function of the yttrium doping level is shown in **Figure 5a** showing a peak in the dielectric constant for YSZ with 5 mol. % yttrium doping. This peak corresponds to the highest fraction of the cubic YSZ phase.

Figure 5b shows the band gap versus the static dielectric constant of solution-processed gate dielectric films along with a large number of dielectric films deposited using vacuum-based techniques,[8,78-84] demonstrating the attractive positioning in terms of band gap and dielectric constant of our YSZ.

Also, as shown in **Figure 5c,** a minimum leakage current density for the highest dielectric constant is ~0.3 nA/cm^2 at an electric field of 2 MV/cm further confirms the deposition of YSZ films of superior high dielectric strength and dielectric constant compared to that of other dielectrics deposited from solutions [8,25,79,81,84-90]. The same applies to the dielectric constant values

ACCEPTED MANUSCRIPT

APL Materials

This is the author's peer reviewed, accepted manuscript. However, the online version of record will be different from this version once it has been copyedited and typeset.
PLEASE CITE THIS ARTICLE AS DOI:10.1063/5.0079195

AIP Publishing

of those films deposited by vacuum based techniques on various substrates and substrate temperatures. [27,57,91-96]

The Poole-Frenkel plots for YSZ with different yttrium doping levels are shown in **Figure 6** indicating the Poole-Frenkel effect as the dominant conduction mechanism at room temperature, an expected finding for such relatively thick and low leakage current insulator.[97]

Next, the performance of the YSZ as a gate dielectric in bottom-gate top-contact thin films transistors was explored. The In_2O_3 semiconducting channel layer was previously characterized independently and found to be the cubic phase with lattice constant *a* of 10.0949 Å and band gap of 3.58 eV[80] (**Figure S4**).

A set of transfer characteristics (operating at saturation) are illustrated in **Figure 7a.** As illustrated in **Figure 7b** and **Figure 7c**, a high electron mobility of ~36 cm^2/Vs and high on/off current modulation ratio, in excess of 10^7, were measured for the TFTs incorporating YSZ with 5 mol.% yttrium doping. An interfacial trap density of ~10^{12} cm^{-2} was measured for the TFT at the optimal 5 mol.% yttrium level, again indicative of a high-quality interface between the YSZ and In_2O_3. The variation of the conduction threshold **(Figure 7d**) is consistent with both the variation in the dielectric constant, k and D_{it}. The variation of the onset-of-conduction or conduction threshold is predominantly determined by the voltage drop across the YSZ gate-dielectric (V_{ins}) and the voltage drop across the YSZ-semiconductor interface (V_{int}). The latter is a function of the interface state density (D_{it}) whereas the former a function of the dielectric constant, k. As seen in Fig. 7d, D_{it} (and hence V_{int}) reaches its minimum and k its highest value at an yttrium doping level of 5 mol.% as seen in **Figure 5a**, giving rise to a low conduction threshold.

In summary, we fabricated YSZ thin films with a range of yttrium concentrations, by spraying pyrolysis of blends of metalorganic precursor solutions of zirconium (IV) 2,4-pentanedionate) with Y_2O_3 nanoparticles dispersions in air at 400°C. An optimum composition

ACCEPTED MANUSCRIPT
APL Materials
This is the author's peer reviewed, accepted manuscript. However, the online version of record will be different from this version once it has been copyedited and typeset.
PLEASE CITE THIS ARTICLE AS DOI:10.1063/5.0079195
AIP Publishing

corresponding to 5 mol. % of yttrium in YSZ gives a wide band gap (5.96 eV), high dielectric constant (26), low leakage current (0.3 nA cm^{-2} at 2 MV/cm), and smooth surface (R_{rms} 0.5 nm), over a large substrate area of ~256 cm^2. Furthermore, In_2O_3-based TFTs were fabricated by spraying an In_2O_3 semiconducting channel onto the optimum YSZ dielectric film. The TFTs showed excellent characteristics, such as high electron mobility (36 cm^2 V^{-1} s^{-1}), high on/off current modulation ratio (10^7) low interfacial trap density states ($<10^{12}$ cm^{-2}), enhancement mode operation and negligible hysteresis. Finally, the high quality YSZ films made using the simple, low temperature and low-cost process could have potential applications in thermal barrier coatings, fuel cells, and other electrochemical devices.

Supporting Information

Supporting Information is available from the AIP Publishing or from the author. The data that support the findings of this study are available from the corresponding author upon reasonable request.

Acknowledgements

G. A. is grateful for support from the Royal Academy of Engineering and Leverhulme Trust grant LTSRF1718\14\14, O.V.K. acknowledges the support of Royal Society (Paul Instrument Fund) and EPSRC grants EP/G06556X/1 and feasibility funding via EP/P006973/1. J.L.M.D. thanks the Royal Academy of Engineering - CIET1819_24 grant.

Author Declarations - Conflict of interest

The authors have no conflicts to disclose.

APL Materials
ACCEPTED MANUSCRIPT
This is the author's peer reviewed, accepted manuscript. However, the online version of record will be different from this version once it has been copyedited and typeset.
PLEASE CITE THIS ARTICLE AS DOI:10.1063/5.0079195
AIP Publishing

References

[1] K. Nomura, H. Ohta, K. Ueda, T. Kamiya, M. Hirano, and H. Hosono, Science (80-.). **300**, 1269 (2003).

[2] K. Nomura, H. Ohta, A. Takagi, T. Kamiya, M. Hirano, and H. Hosono, Nature **432**, 488 (2004).

[3] E. Fortunato, P. Barquinha, and R. Martins, Adv. Mater. **24**, 2945 (2012).

[4] E. Fortunato, P. Barquinha, A. Pimentel, L. Pereira, G. Gonçalves, and R. Martins, Phys. Status Solidi - Rapid Res. Lett. **1**, R34 (2007).

[5] K.K. Pandey, N. Garg, a K. Mishra, and S.M. Sharma, J. Phys. Conf. Ser. **377**, 012006 (2012).

[6] N.L. Dehuff, E.S. Kettenring, D. Hong, H.Q. Chiang, J.F. Wager, R.L. Hoffman, C.H. Park, and D.A. Keszler, J. Appl. Phys. **97**, 064505 (2005).

[7] M. Esro, G. Vourlias, C. Somerton, W.I. Milne, and G. Adamopoulos, Adv. Funct. Mater. **25**, 134 (2015).

[8] M. Esro, O. Kolosov, V. Stolojan, P.J. Jones, W.I. Milne, and G. Adamopoulos, Adv. Electron. Mater. **3**, 1700025 (2017).

[9] A. Bashir, P.H. Wöbkenberg, J. Smith, J.M. Ball, G. Adamopoulos, D.D.C. Bradley, and T.D. Anthopoulos, Adv. Mater. **21**, 2226 (2009).

[10] S.R. Thomas, G. Adamopoulos, Y.-H. Lin, H. Faber, L. Sygellou, E. Stratakis, N. Pliatsikas, P.A. Patsalas, and T.D. Anthopoulos, Appl. Phys. Lett. **105**, (2014).

[11] Y.-H. Lin, S.R. Thomas, H. Faber, R. Li, M.A. McLachlan, P.A. Patsalas, and T.D. Anthopoulos, Adv. Electron. Mater. **2**, 1600070 (2016).

[12] S.R. Thomas, P. Pattanasattayavong, and T.D. Anthopoulos, Chem. Soc. Rev. **42**, 6910 (2013).

[13] K.K. Banger, Y. Yamashita, K. Mori, R.L. Peterson, T. Leedham, J. Rickard, and H. Sirringhaus, Nat. Mater. **10**, 45 (2011).

[14] M.-G. Kim, M.G. Kanatzidis, A. Facchetti, and T.J. Marks, Nat. Mater. **10**, 382 (2011).

APL Materials
ACCEPTED MANUSCRIPT
This is the author's peer reviewed, accepted manuscript. However, the online version of record will be different from this version once it has been copyedited and typeset.
PLEASE CITE THIS ARTICLE AS DOI:10.1063/5.0079195
AIP Publishing

[15] W. Huang, X. Yu, L. Zeng, B. Wang, A. Takai, G. Di Carlo, M.J. Bedzyk, T.J. Marks, and A. Facchetti, ACS Appl. Mater. Interfaces **13**, 3445 (2021).

[16] X. Zhuang, S. Patel, C. Zhang, B. Wang, Y. Chen, H. Liu, V.P. Dravid, J. Yu, Y.-Y. Hu, W. Huang, A. Facchetti, and T.J. Marks, J. Am. Chem. Soc. **142**, 12440 (2020).

[17] R.M. Wallace and G.D. Wilk, Crit. Rev. Solid State Mater. Sci. **28**, 231 (2003).

[18] G.D. Wilk, R.M. Wallace, and J.M. Anthony, J. Appl. Phys. **89**, 5243 (2001).

[19] J.D. Plummer and P.B. Griffin, Proc. IEEE **89**, 240 (2001).

[20] J. Robertson and C.W. Chen, Appl. Phys. Lett. **74**, 1168 (1999).

[21] J. Robertson, Reports Prog. Phys. **69**, 327 (2006).

[22] J.A. Kittl, K. Opsomer, M. Popovici, N. Menou, B. Kaczer, X.P. Wang, C. Adelmann, M.A. Pawlak, K. Tomida, A. Rothschild, B. Govoreanu, R. Degraeve, M. Schaekers, M. Zahid, A. Delabie, J. Meersschaut, W. Polspoel, S. Clima, G. Pourtois, W. Knaepen, C. Detavernier, V.V. Afanas'ev, T. Blomberg, D. Pierreux, J. Swerts, P. Fischer, J.W. Maes, D. Manger, W. Vandervorst, T. Conard, A. Franquet, P. Favia, H. Bender, B. Brijs, S. Van Elshocht, M. Jurczak, J. Van Houdt, and D.J. Wouters, Microelectron. Eng. **86**, 1789 (2009).

[23] R. Engel-Herbert, Y. Hwang, J. Cagnon, and S. Stemmer, Appl. Phys. Lett. **95**, 062908 (2009).

[24] D.M. Hausmann, E. Kim, J. Becker, and R.G. Gordon, Chem. Mater. **14**, 4350 (2002).

[25] S.T. Meyers, J.T. Anderson, D. Hong, C.M. Hung, J.F. Wager, and D.A. Keszler, Chem. Mater. **19**, 4023 (2007).

[26] M. Hartmanova, K. Gmucova, and I. Thurzo, Solid State Ionics **130**, 105 (2000).

[27] S.H. Jeong, I.S. Bae, Y.S. Shin, S.B. Lee, H.T. Kwak, and J.H. Boo, Thin Solid Films **475**, 354 (2005).

[28] S.J. Wang, C.K. Ong, S.Y. Xu, P. Chen, W.C. Tjiu, A.C.H. Huan, W.J. Yoo, J.S. Lim, W. Feng, and W.K. Choi, Semicond. Sci. Technol. **16**, L13 (2001).

ACCEPTED MANUSCRIPT
APL Materials
This is the author's peer reviewed, accepted manuscript. However, the online version of record will be different from this version once it has been copyedited and typeset.
PLEASE CITE THIS ARTICLE AS DOI:10.1063/5.0079195
AIP Publishing

[29] A. Sharma, M. Varshney, H.J. Shin, Y. Kumar, S. Gautam, and K.H. Chae, Chem. Phys. Lett. **592**, 85 (2014).

[30] A. Benyagoub, F. Couvreur, S. Bouffard, F. Levesque, C. Dufour, and E. Paumier, Nucl. Instruments Methods Phys. Res. Sect. B Beam Interact. with Mater. Atoms **175–177**, 417 (2001).

[31] M. Kuwabara, T. Murakami, M. Ashizuka, Y. Kubota, and T. Tsukidate, J. Mater. Sci. Lett. **4**, 467 (1985).

[32] M. Hartmanová, I. Thurzo, M. Jergel, J. Bartoš, F. Kadlec, V. Zelezný, D. Tunega, F. Kundracik, S. Chromik, and M. Brunel, J. Mater. Sci. **33**, 969 (1998).

[33] M.Y. Arsent'ev, M. V. Kalinina, P.A. Tikhonov, L. V. Morozova, A.S. Kovalenko, N.Y. Koval'ko, I.I. Khlamov, and O.A. Shilova, Glas. Phys. Chem. **40**, 362 (2014).

[34] I. Kosacki, T. Suzuki, V. Petrovsky, and H.U. Anderson, Solid State Ionics **136**–**137**, 1225 (2000).

[35] M. Yashima, K. Morimoto, N. Ishizawa, and M. Yoshimura, J. Am. Ceram. Soc. **76**, 2865 (1993).

[36] D.L. Porter and A.H. Heuer, J. Am. Ceram. Soc. **62**, 298 (1979).

[37] B.C. Muddle and R.H.J. Hannink, J. Am. Ceram. Soc. **69**, 547 (1986).

[38] E.N.S. Muccillo and M. Kleitz, J. Eur. Ceram. Soc. **16**, 453 (1996).

[39] S.P.S. Badwal, Solid State Ionics **52**, 23 (1992).

[40] D. Michel, F. Faudot, E. Gaffet, and L. Mazerolles, J. Am. Ceram. Soc. **76**, 2884 (1993).

[41] M. Kilo, M.A. Taylor, C. Argirusis, G. Borchardt, B. Lesage, S. Weber, S. Scherrer, H. Scherrer, M. Schroeder, and M. Martin, J. Appl. Phys. **94**, 7547 (2003).

[42] N. Bonanos, R.K. Slotwinski, B.C.H. Steele, and E.P. Butler, J. Mater. Sci. **19**, 785 (1984).

[43] V.P. Dravid, V. Ravikumar, M.R. Notis, C.E. Lyman, G. Dhalenne, and A. Revcolevschi, ChemInform **26**, 2758 (2010).

[44] M. Johansson, T. Mattisson, and A. Lyngfelt, Chem. Eng. Res. Des. **84**, 807 (2006).

[45] P. Simoncic and A. Navrotsky, J. Am. Ceram. Soc. **90**, 2143 (2007).

ACCEPTED MANUSCRIPT
APL Materials
This is the author's peer reviewed, accepted manuscript. However, the online version of record will be different from this version once it has been copyedited and typeset.
PLEASE CITE THIS ARTICLE AS DOI:10.1063/5.0079195
AIP Publishing

[46] B. Ksapabutr, T. Chalermkiti, S. Wongkasemjit, and M. Panapoy, Thin Solid Films **518**, 6518 (2010).

[47] G.C.C. Costa and R. Muccillo, Solid State Ionics **179**, 1219 (2008).

[48] G. Sirinakis, R. Siddique, I. Manning, P.H. Rogers, and M.A. Carpenter, J. Phys. Chem. B **110**, 13508 (2006).

[49] L.B. Chen, Surf. Rev. Lett. **13**, 535 (2007).

[50] U. Anselmi-Tamburini, J.N. Woolman, and Z.A. Munir, Adv. Funct. Mater. **17**, 3267 (2007).

[51] E.W. Leib, R.M. Pasquarelli, J.J. do Rosário, P.N. Dyachenko, S. Döring, A. Puchert, A.Y. Petrov, M. Eich, G.A. Schneider, R. Janssen, H. Weller, and T. Vossmeyer, J. Mater. Chem. C **4**, 62 (2016).

[52] G. Marcaud, S. Matzen, C. Alonso-Ramos, X. Le Roux, M. Berciano, T. Maroutian, G. Agnus, P. Aubert, L. Largeau, V. Pillard, S. Serna, D. Benedikovic, C. Pendenque, E. Cassan, D. Marris-Morini, P. Lecoeur, and L. Vivien, Phys. Rev. Mater. **2**, 035202 (2018).

[53] C.L. Hardin, Y. Kodera, S.A. Basun, D.R. Evans, and J.E. Garay, Opt. Mater. Express **3**, 893 (2013).

[54] K.K. Gopalan, D. Rodrigo, B. Paulillo, K.K. Soni, and V. Pruneri, Adv. Opt. Mater. **7**, 1800966 (2019).

[55] J.W. Reiner, A.M. Kolpak, Y. Segal, K.F. Garrity, S. Ismail-Beigi, C.H. Ahn, and F.J. Walker, Adv. Mater. **22**, 2919 (2010).

[56] G. Garcia, J. Caro, J. Santiso, J.A. Pardo, A. Figueras, and A. Abrutis, Chem. Vap. Depos. **9**, 279 (2003).

[57] S.Y. Chun and N. Mizutani, Appl. Surf. Sci. **171**, 82 (2001).

[58] J.H. Shim, C.C. Chao, H. Huango, and F.B. Prinz, Chem. Mater. **19**, 3850 (2007).

[59] C. Bernay, A. Ringuedé, P. Colomban, D. Lincot, and M. Cassir, J. Phys. Chem. Solids **64**, 1761

ACCEPTED MANUSCRIPT
APL Materials
This is the author's peer reviewed, accepted manuscript. However, the online version of record will be different from this version once it has been copyedited and typeset.
PLEASE CITE THIS ARTICLE AS DOI: 10.1063/5.0079195
AIP Publishing

(2003).

[60] S.G. Kim, S.P. Yoon, S.W. Nam, S.H. Hyun, and S.A. Hong, J. Power Sources **110**, 222 (2002).

[61] X. Xu, C. Xia, S. Huang, and D. Peng, Ceram. Int. **31**, 1061 (2005).

[62] C. Viazzi, J.-P. Bonino, F. Ansart, and A. Barnabé, J. Alloys Compd. **452**, 377 (2008).

[63] A. Infortuna, A.S. Harvey, and L.J. Gauckler, Adv. Funct. Mater. **18**, 127 (2008).

[64] A. Cavallaro, M. Burriel, J. Roqueta, A. Apostolidis, A. Bernardi, A. Tarancón, R. Srinivasan, S.N. Cook, H.L. Fraser, and J.A. Kilner, Solid State Ionics **181**, 592 (2010).

[65] S. Heiroth, R. Ghisleni, T. Lippert, J. Michler, and A. Wokaun, Acta Mater. **59**, 2330 (2011).

[66] S. Heiroth, T. Lippert, A. Wokaun, M. Döbeli, J.L.M. Rupp, B. Scherrer, and L.J. Gauckler, J. Eur. Ceram. Soc. **30**, 489 (2010).

[67] H. Huang, M. Nakamura, P. Su, R. Fasching, Y. Saito, and F.B. Prinz, J. Electrochem. Soc. **154**, B20 (2006).

[68] S. Sønderby, B.H. Christensen, K.P. Almtoft, L.P. Nielsen, and P. Eklund, Surf. Coatings Technol. **281**, 150 (2015).

[69] M. Sillassen, P. Eklund, N. Pryds, E. Johnson, U. Helmersson, and J. Bøttiger, Adv. Funct. Mater. **20**, 2071 (2010).

[70] P. Coddet, M.L. Amany, J. Vulliet, A. Caillard, and A.L. Thomann, Surf. Coatings Technol. **357**, 103 (2019).

[71] H. Jiang, R.I. Gomez-Abal, P. Rinke, and M. Scheffler, Phys. Rev. B - Condens. Matter Mater. Phys. **81**, 085119 (2010).

[72] P. Camagni, P. Galinetto, G. Samoggia, and N. Zema, Solid State Commun. **83**, 943 (1992).

[73] N. Nicoloso, A. Löbert, and B. Leibold, Sensors Actuators B. Chem. **8**, 253 (1992).

[74] J.-M. Costantini, F. Beuneu, D. Gourier, C. Trautmann, G. Calas, and M. Toulemonde, J. Phys. Condens. Matter **16**, 3957 (2004).

APL Materials ACCEPTED MANUSCRIPT
This is the author's peer reviewed, accepted manuscript. However, the online version of record will be different from this version once it has been copyedited and typeset.
PLEASE CITE THIS ARTICLE AS DOI:10.1063/5.0079195
AIP Publishing

[75] P. Bouvier, E. Djurado, G. Lucazeau, and T. Le Bihan, Phys. Rev. B **62**, 8731 (2000).

[76] T. Götsch, W. Wallisch, M. Stöger-Pollach, B. Klötzer, and S. Penner, AIP Adv. **6**, 025119 (2016).

[77] G.P. Cousland, X.Y. Cui, A.E. Smith, A.P.J. Stampfl, and C.M. Stampfl, J. Phys. Chem. Solids **122**, 51 (2018).

[78] J. Robertson and R.M. Wallace, Mater. Sci. Eng. R Reports **88**, 1 (2015).

[79] M. Esro, G. Vourlias, C. Somerton, W.I. Milne, and G. Adamopoulos, Adv. Funct. Mater. **25**, 134 (2015).

[80] K. Paxinos, G. Antoniou, D. Afouxenidis, A. Mohamed, U. Dikko, I. Tsitsimpelis, W.I. Milne, A. Nathan, and G. Adamopoulos, Appl. Phys. Lett. **116**, 163505 (2020).

[81] M. Esro, O. Kolosov, P.J. Jones, W.I. Milne, and G. Adamopoulos, ACS Appl. Mater. Interfaces **9**, 529 (2017).

[82] D. Afouxenidis, R. Mazzocco, G. Vourlias, P.J. Livesley, A. Krier, W.I. Milne, O. Kolosov, and G. Adamopoulos, ACS Appl. Mater. Interfaces **7**, 7334 (2015).

[83] M. Esro, R. Mazzocco, G. Vourlias, O. Kolosov, A. Krier, W.I. Milne, and G. Adamopoulos, Appl. Phys. Lett. **106**, (2015).

[84] G. Adamopoulos, S. Thomas, P.H. Wöbkenberg, D.D.C. Bradley, M.A. McLachlan, and T.D. Anthopoulos, Adv. Mater. **23**, 1894 (2011).

[85] M. Esro, G. Vourlias, C. Somerton, W.I. Milne, and G. Adamopoulos, Adv. Funct. Mater. **25**, 134 (2015).

[86] D. Afouxenidis, R. Mazzocco, G. Vourlias, P.J. Livesley, A. Krier, W.I. Milne, O. Kolosov, and G. Adamopoulos, ACS Appl. Mater. Interfaces **7**, 7334 (2015).

[87] M. Esro, R. Mazzocco, G. Vourlias, O. Kolosov, a. Krier, W.I. Milne, and G. Adamopoulos, Appl. Phys. Lett. **106**, 203507 (2015).

ACCEPTED MANUSCRIPT
APL Materials
This is the author's peer reviewed, accepted manuscript. However, the online version of record will be different from this version once it has been copyedited and typeset.
PLEASE CITE THIS ARTICLE AS DOI:10.1063/5.0079195
AIP Publishing

[88] G. Adamopoulos, S. Thomas, D.D.C. Bradley, M.A. McLachlan, and T.D. Anthopoulos, Appl. Phys. Lett. **98**, 123503 (2011).

[89] J.-W. Jo, Y.-H. Kim, J. Park, J.S. Heo, S. Hwang, W.-J. Lee, M.-H. Yoon, M.-G. Kim, and S.K. Park, ACS Appl. Mater. Interfaces **9**, 35114 (2017).

[90] K.C. Lau and B.I. Dunlap, J. Phys. Condens. Matter **21**, 145402 (2009).

[91] D.I. Shahin, M.J. Tadjer, V.D. Wheeler, A.D. Koehler, T.J. Anderson, C.R. Eddy, and A. Christou, Appl. Phys. Lett. **112**, 042107 (2018).

[92] J. Molina-Reyes, H. Tiznado, G. Soto, M. Vargas-Bautista, D. Dominguez, E. Murillo, D. Sweeney, and J. Read, J. Mater. Sci. Mater. Electron. **29**, 15349 (2018).

[93] A. Dimoulas, G. Mavrou, G. Vellianitis, E. Evangelou, N. Boukos, M. Houssa, and M. Caymax, Appl. Phys. Lett. **86**, 032908 (2005).

[94] S. Horita, M. Watanabe, and A. Masuda, Mater. Sci. Eng. B **54**, 79 (2002).

[95] J. Zhu and Z.G. Liu, Mater. Lett. **57**, 4297 (2003).

[96] A.P. Caricato, G. Barucca, A. Di Cristoforo, G. Leggieri, A. Luches, G. Majni, M. Martino, and P. Mengucci, Appl. Surf. Sci. **248**, 270 (2005).

[97] H. Wong, IEEE Conf. Electron Devices Solid-State Circuits 2007, EDSSC 2007 31 (2007).

APL Materials
ACCEPTED MANUSCRIPT
This is the author's peer reviewed, accepted manuscript. However, the online version of record will be different from this version once it has been copyedited and typeset.
PLEASE CITE THIS ARTICLE AS DOI:10.1063/5.0079195
AIP Publishing

Figure Captions

Figure 1: a) Optical band gap and **b)** Urbach tail energy of YSZ films as a function of the yttrium content in the precursor solution.

Figure 2: a) GIXRD patterns of YSZ films and, **b)** average crystal size and (111) – cubic to (011)-tetragonal peak intensity ratio of YSZ of films with different yttrium doping levels. The solid lines are guides to the eye.

Figure 3: AFM friction image of YSZ surface (topography images inset) with increasing yttrium doping level of **a)** 0 mol.%, **b)** 5 mol.% and **c)** 15 mol%. High resolution cross section UFM images of YSZ, with yttrium content of **d)** 0 mol.%, **e)** 5 mol.% and **f)** mol.15 %. (**Insets**: UFM high resolution images of cross-sectional interfaces of glass/ITO/YSZ/In_2O_3/Al device stacks).

Figure 4: Bode plots of YSZ films with different yttrium doping levels.

Figure 5: a) Dielectric constant of spray coated YSZ as a function of the yttrium doping level, **b)** static dielectric constant versus band gap of selected metal oxide gate dielectrics deposited by spray coating as well as vacuum-based techniques, **c)** leakage current density at 2 MV cm^{-1} of YSZ dielectrics as a function of the yttrium doping level.

Figure 6: a) Current voltage characteristics and **b)** Poole – Frenkel plots of YSZ films with different yttrium doping levels in solution.

Figure 7: **a)** Transfer characteristics at saturation (V_{DS}= 5 V), **b)** electron mobility (TFT structure inset), **c)** on/off current modulation ratio, **d)** interfacial trap density and conduction threshold of In_2O_3 TFTs implementing YSZ dielectrics as a function of the yttrium content in the precursor solution. In all cases, the solid lines guide the eye.

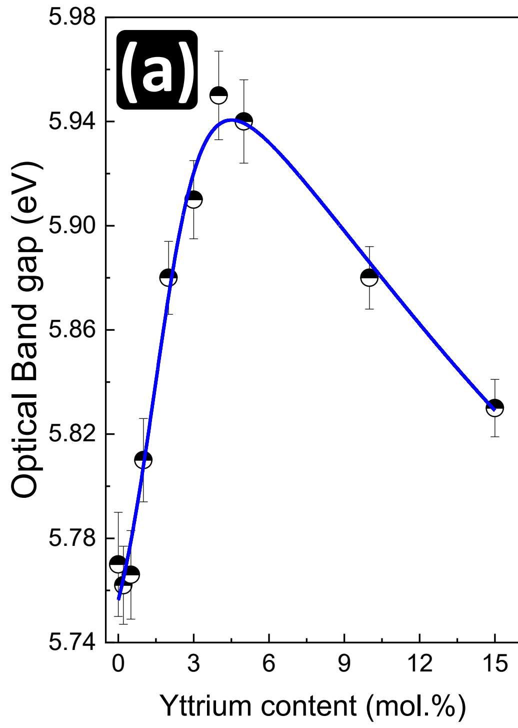
(a)
Optical Band gap (eV)
Yttrium content (mol.%)
5.98
5.94
5.90
5.86
5.82
5.78
5.74
0
3
6
9
12
15

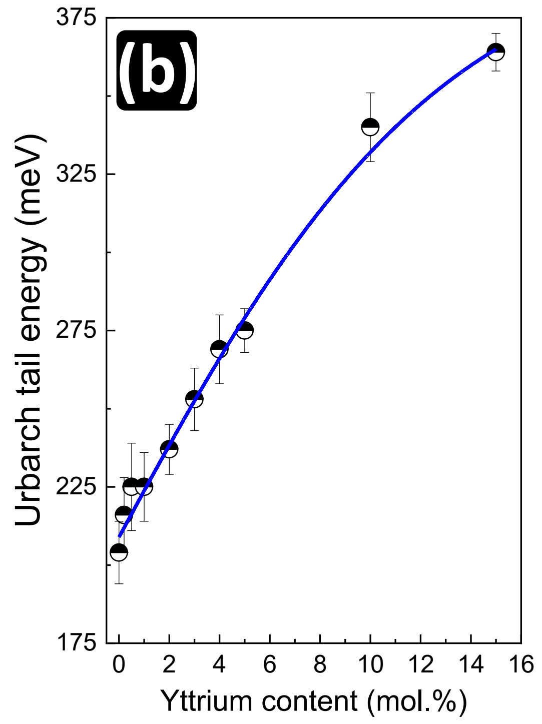
(b)
Urbarch tail energy (meV)
Yttrium content (mol.%)
375
325
275
225
175
0
2
4
6
8
10
12
14
16

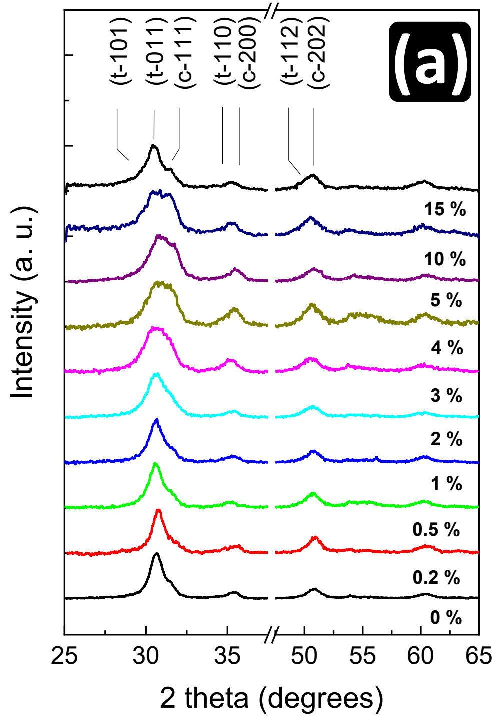
(a)
(t-101)
(t-011)
(c-111)
(t-110)
(c-200)
(t-112)
(c-202)
15 %
10 %
5 %
4 %
3 %
2 %
1 %
0.5 %
0.2 %
0 %
Intensity (a. u.)
2 theta (degrees)
25
30
35
50
55
60
65
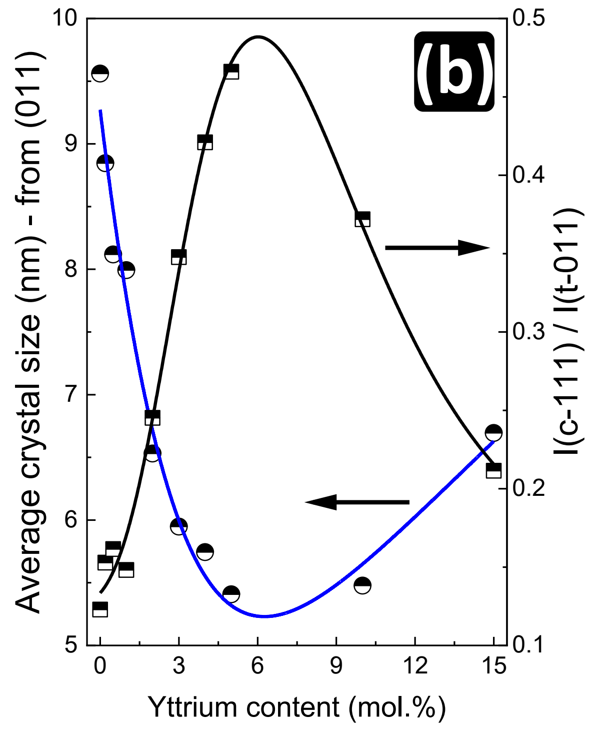
(b)
Average crystal size (nm) - from (011)
I(c-111) / I(t-011)
Yttrium content (mol.%)
10
9
8
7
6
5
0.5
0.4
0.3
0.2
0.1
0
3
6
9
12
15

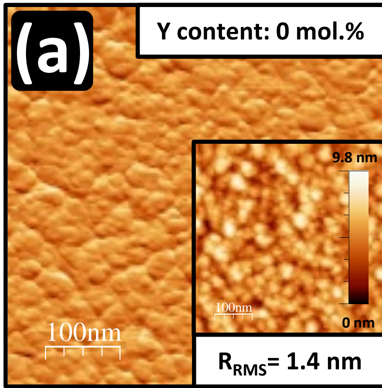
(a)
Y content: 0 mol.%
9.8 nm
0 nm
100nm
100nm
R_{RMS}= 1.4 nm

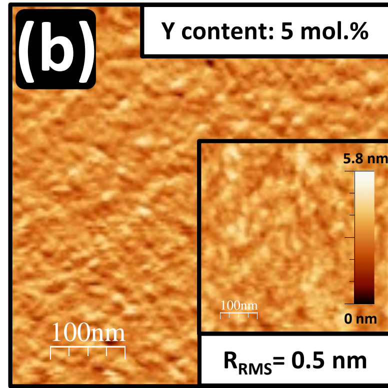
(b)
Y content: 5 mol.%
5.8 nm
0 nm
100nm
100nm
R_{RMS}= 0.5 nm

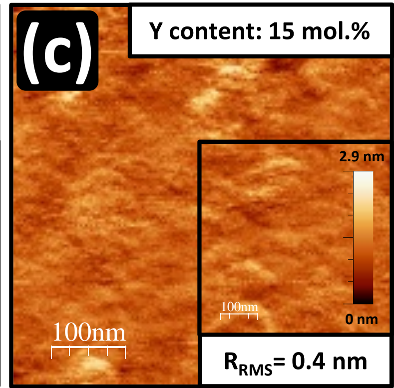
(c)
Y content: 15 mol.%
2.9 nm
0 nm
100nm
100nm
R_{RMS}= 0.4 nm

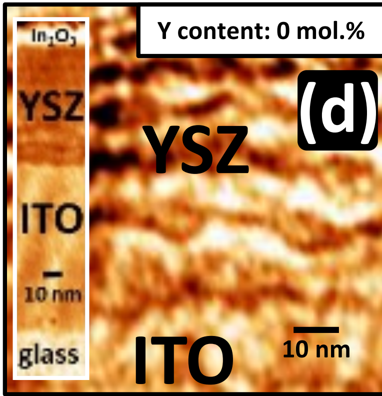
Y content: 0 mol.%
In_2O_3
YSZ
ITO
10 nm
glass
YSZ
(d)
ITO
10 nm

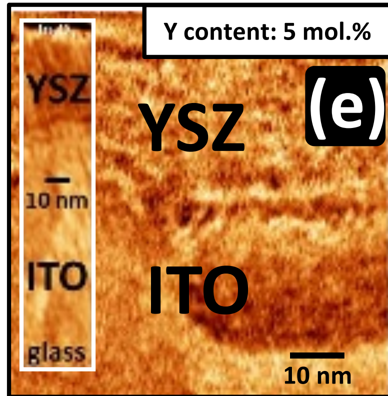
Y content: 5 mol.%
YSZ
10 nm
ITO
glass
YSZ
(e)
ITO
10 nm

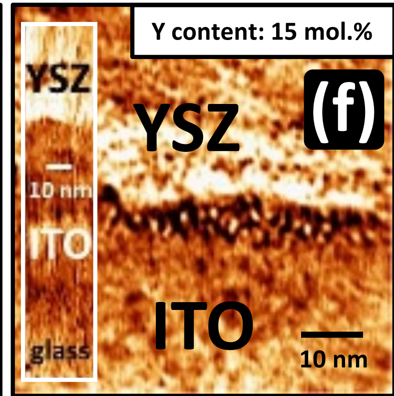
Y content: 15 mol.%
YSZ
10 nm
ITO
glass
YSZ
(f)
ITO
10 nm

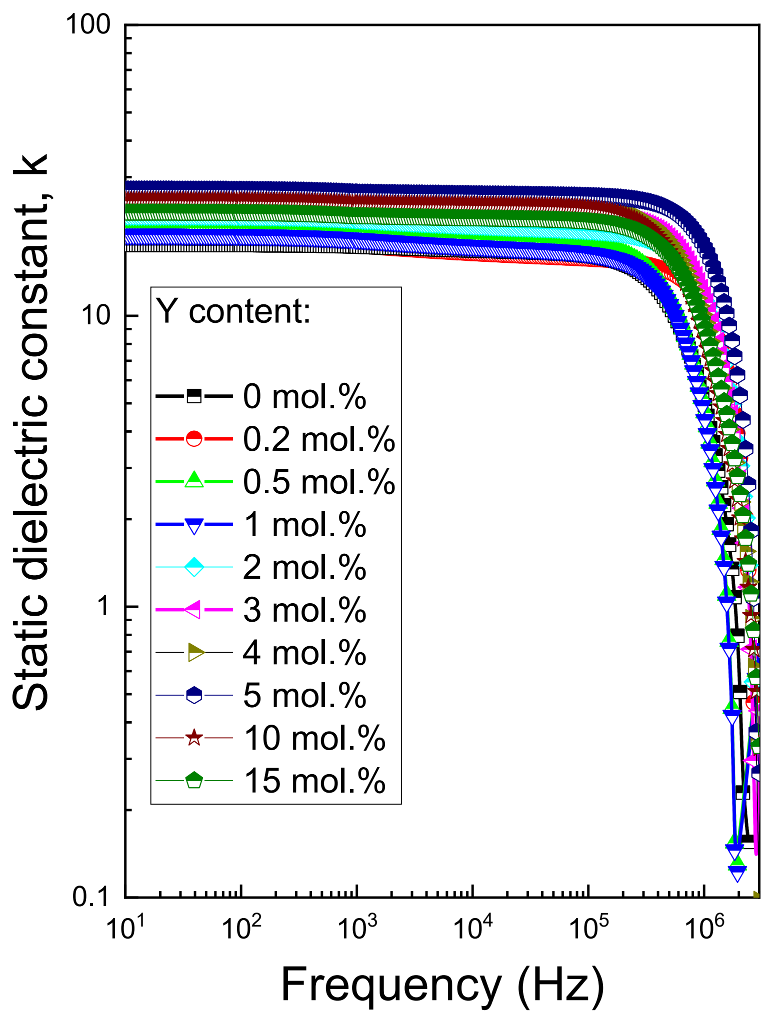
Static dielectric constant, k
Frequency (Hz)
Y content:
0 mol.%
0.2 mol.%
0.5 mol.%
1 mol.%
2 mol.%
3 mol.%
4 mol.%
5 mol.%
10 mol.%
15 mol.%
100
10
1
0.1
10^1
10^2
10^3
10^4
10^5
10^6

Static dielectric constant, k

100

10

1

0.1

10^1 10^2 10^3 10^4 10^5 10^6

Frequency (Hz)

Y content:

0 mol.%

0.2 mol.%

0.5 mol.%

1 mol.%

2 mol.%

3 mol.%

4 mol.%

5 mol.%

10 mol.%

15 mol.%

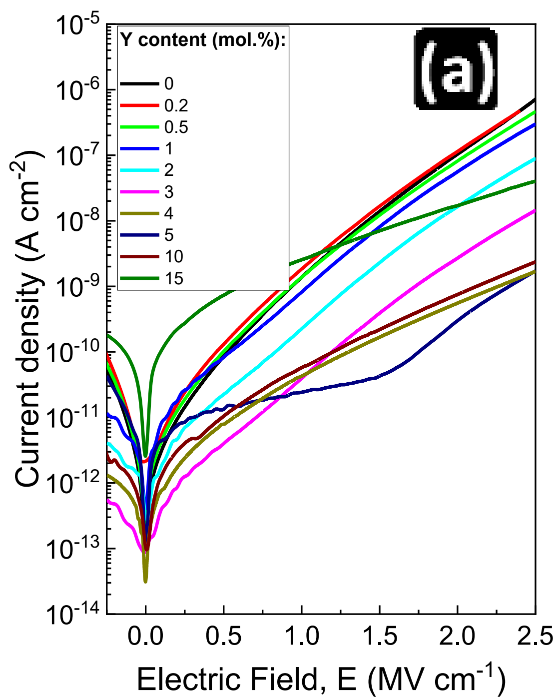
(a)
Y content (mol.%):
0
0.2
0.5
1
2
3
4
5
10
15
Current density (A cm^{-2})
Electric Field, E (MV cm^{-1})

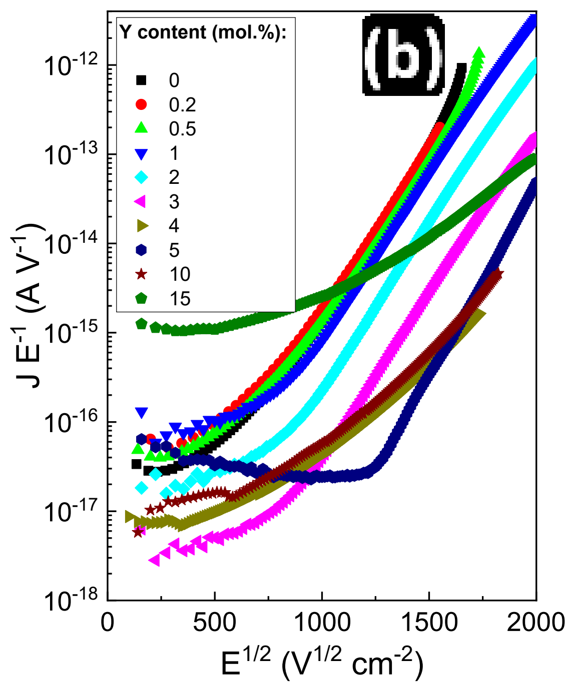
(b)
Y content (mol.%):
0
0.2
0.5
1
2
3
4
5
10
15
J E^{-1} (A V^{-1})
E$^{1/2}$ (V$^{1/2}$ cm^{-2})

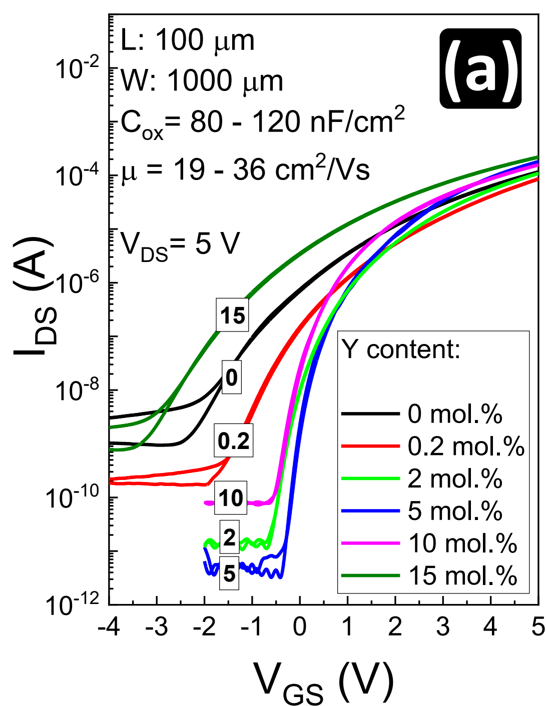

L: 100 μm
W: 1000 μm
C_ox= 80 - 120 nF/cm²
μ = 19 - 36 cm²/Vs
V_DS= 5 V
(a)
15
0
0.2
10
2
5
Y content:
0 mol.%
0.2 mol.%
2 mol.%
5 mol.%
10 mol.%
15 mol.%
I_DS (A)
V_GS (V)

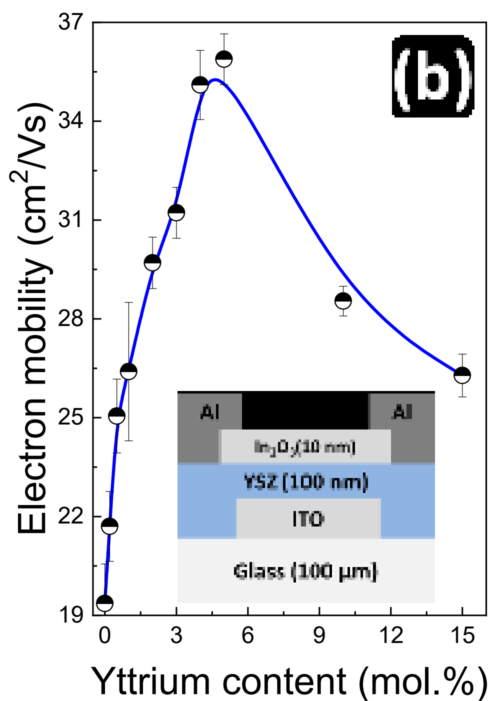

(b)
Electron mobility (cm²/Vs)
Yttrium content (mol.%)
Al
Al
In₂O₃(10 nm)
YSZ (100 nm)
ITO
Glass (100 μm)

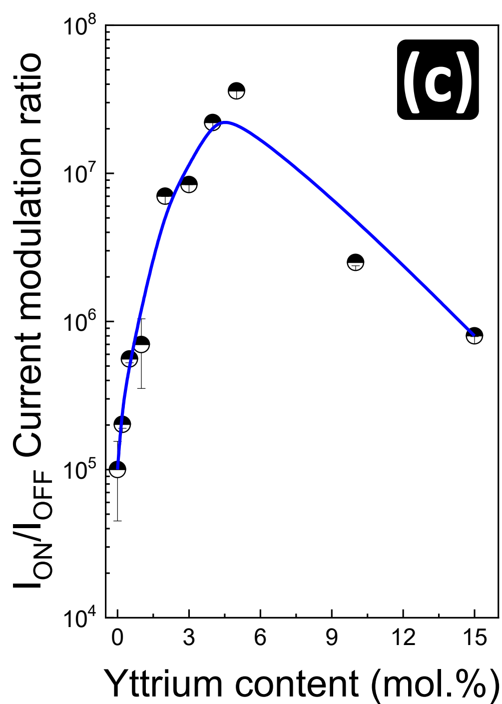

(c)
I_ON/I_OFF Current modulation ratio
Yttrium content (mol.%)

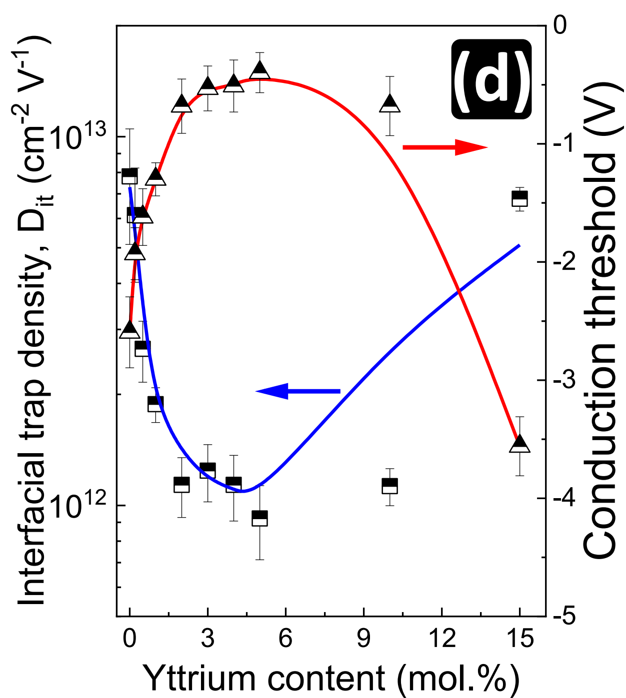

(d)
Interfacial trap density, D_it (cm⁻² V⁻¹)
Conduction threshold (V)
Yttrium content (mol.%)